Changes in the variability of global land precipitation

Fubao Sun,[1,2] Michael L. Roderick,[1,2,3] and Graham D. Farquhar[1,2]

Received 30 July 2012; revised 24 August 2012; accepted 27 August 2012; published 2 October 2012.

[1] In our warming climate there is a general expectation that the variability of precipitation (*P*) will increase at daily, monthly and inter-annual timescales. Here we analyse observations of monthly *P* (1940–2009) over the global land surface using a new theoretical framework that can distinguish changes in global *P* variance between space and time. We report a near-zero temporal trend in global mean *P*. Unexpectedly we found a reduction in global land *P* variance over space and time that was due to a redistribution, where, on average, the dry became wetter while wet became drier. Changes in the *P* variance were not related to variations in temperature. Instead, the largest changes in *P* variance were generally found in regions having the largest aerosol emissions. Our results combined with recent modelling studies lead us to speculate that aerosol loading has played a key role in changing the variability of *P*. **Citation:** Sun, F., M. L. Roderick, and G. D. Farquhar (2012), Changes in the variability of global land precipitation, *Geophys. Res. Lett.*, *39*, L19402, doi:10.1029/2012GL053369.

1. Introduction

[2] In many instances, e.g., agricultural and natural ecosystems, and for water resources planning, changes in the variability (or upper/lower extremes) of precipitation (*P*) (e.g., floods and droughts) over the land surface can be as important as changes in the mean [*Easterling et al.*, 2000a, 2000b; *Rodríguez-Iturbe and Porporato*, 2004; *Porporato et al.*, 2004]. With global warming, climate models project increased *P* variability in most regions at daily [*O'Gorman and Schneider*, 2009], monthly [*Benestad*, 2006] and inter-annual [*Boer*, 2009; *Held and Soden*, 2006; *Rind et al.*, 1989; *Wetherald*, 2010] timescales. Expectations are for *P* extremes in storm events to increase with the saturation vapour pressure in the atmosphere ($\sim$7% K^{-1}) [*Trenberth et al.*, 2003]. Energetic constraints limit the increase of global *P* ($\sim$2% K^{-1}) [*Allen and Ingram*, 2002] so that the mean time interval between successive storms is also expected to increase [*Trenberth et al.*, 2003] by $\sim$5% K^{-1}. An increase in *P* extremes in storm events due to warming is relevant over short time scales (minutes-hours) and relates directly to the occurrence of floods [*Allan and Soden*, 2008; *O'Gorman and Schneider*, 2009]. However, care is needed before applying that logic to the longer periods (months-years) of relevance to droughts since relative changes in the dry period length would be small. For example, Chicago's mean annual *P* (910 mm) falls in $\sim$660 hours leaving dry the remaining 8100 hours [*Eagleson*, 2002]. If it fell in 5% less time the dry period length would increase by $\sim$0.4% (=0.05 $\times$ 660/8100). Even halving the total duration of storms and thereby doubling the average storm intensity would still only increase the dry period by 4%. Hence, a change in the total storm duration does not provide guidance on changes in longer term *P* variability on time scales relevant to droughts.

[3] Long-term spatial databases at monthly resolution are available to evaluate changes in *P* variability on timescales relevant to droughts. In terms of generic expectations we note that *P* cannot be less than zero and the simplest model is for local-scale variability in *P* to increase (decrease) with increases (decreases) in the local-scale mean *P* [*Groisman et al.*, 1999; *Rind et al.*, 1989]. Observations over the past 50 years show little variation in global mean *P* [*Huffman et al.*, 2009] for periods longer than the turnover time of water in the atmosphere ($\sim$10 days). Hence, over monthly (and longer timescales), any increase in *P* in a given region must have been roughly balanced by decreases elsewhere such that the global *P* remained near constant. Thus, when expressed in terms of precipitation the "wet get wetter and dry get drier" idea [*Chou et al.*, 2007; *Trenberth*, 2011; *Held and Soden* 2006] can be interpreted to imply an increase in the temporal variance in wet regions (since *P* is supposed to increase there) coupled with a decrease in dry regions (since *P* is supposed to decrease there) that could balance leaving little overall temporal change in *P* variability. However, such local changes also require a redistribution of *P* and in the wet-get-wetter dry-get-drier scenario there would also be an accompanying increase in the spatial variance. The key point is that any analysis technique that only examines the changes over time at individual grid-boxes will ignore this spatial component and therefore ignore a potentially important change in the overall climate.

[4] Inspired by the analysis of variance method [*von Storch and Zwiers*, 1999; *Wilks*, 2011], we recently developed a general approach that partitions the overall variance, called the grand variance, into separate spatial and temporal components [*Sun et al.*, 2010]. This new approach can be applied to any space-time database and does not require assumptions about the independence of the data. (See the mathematical derivation in *Sun et al.* [2010].) Here we use the same gridded databases that are already in widespread use. For each decade, we first lump space and time to form one empirical distribution and calculate the grand variance. Following that we separately calculate the temporal variance of each grid-box and also calculate the spatial variance across all grid-boxes. The innovation is that the method

[1]Research School of Biology, Australian National University, Canberra, ACT, Australia.
[2]Australian Research Council Centre of Excellence for Climate System Science, Sydney, New South Wales, Australia.
[3]Research School of Earth Sciences, Australian National University, Canberra, ACT, Australia.

Corresponding author: M. L. Roderick, Research School of Biology, Australian National University, Canberra, ACT 0200, Australia. (michael.roderick@anu.edu.au)

0094-8276/12/2012GL053369

describes how the separate spatial and temporal components are added to equal the grand variance. This new procedure has the advantage that the sources of variation, whether through space, or through time, can be disentangled [*Sun et al.*, 2010]. Here we use that technique to examine changes in P variability in long-term monthly observations.

[5] Data on oceanic P are currently only available from 1979 [*Huffman et al.*, 2009; *Xie and Arkin*, 1997] with many unresolved issues in their use for trend analysis [*Yin et al.*, 2004] (see Section S1 in Text S1 in the auxiliary material).[1] However, the critical impacts of changes in P variability (agriculture, water resources) occur over land. We use global land-based (2.5° × 2.5°) observations in seven monthly databases: GPCC(1901–2009) [*Rudolf and Schneider*, 2005], CRU(1901–2006) [*Mitchell and Jones*, 2005], GPCP(1979–2008) [*Huffman et al.*, 2009], CMAP (1979–2008) [*Xie and Arkin*, 1997], the database compiled by *Dai et al.* [1997] (1920–1995), GHCN (1940–2009, 5° × 5°) [*Peterson and Vose*, 1997], and VASClimO [*Rudolf and Schneider*, 2005] (1951–2000) (see Section S1.1 in Text S1). The VASClimO database used a mostly fixed number of P measurement stations over time [*Rudolf and Schneider*, 2005] (Figure S6a in Text S1) and we adopted that as a reference. To further minimise interpolation problems (see Section S1.3 in Text S1) we use the GPCC metadata to define a spatial mask (fixed over the entire period, Figure S6b in Text S1) by those grid-boxes having at least one measurement site for 90% of the months over the 1951–2000 (VASClimO) period. We also tested other spatial masks using more stringent criteria but the same conclusions held (see Figures S6 and S7 in Text S1). The final mask includes 1,987 grid-boxes (∼69% of global land area excl. Antarctica) and was used to calculate the grand mean (μ_g) and grand variance (σ_g^2) for each successive decade for all seven databases. The different databases gave nearly identical results for the period 1940–2009 (Figures S7–S11 in Text S1). All subsequent results use the mask derived from the GPCC observations (1940–2009).

2. Results

[6] We find that μ_g has a near-zero trend (Figure 1a) while σ_g^2 has a decline of ∼6% (1940–1999, p = 0.003, Mann-Kendall Test) before an increase of ∼5% in the final decade (2000–2009) giving an overall decline (Figure 1b). The 99 Percentile ($P_{0.99}$, Figure 1c), calculated from the empirical distribution lumping space and time [*Allan and Soden*, 2008; *Allen and Ingram*, 2002; *O'Gorman and Schneider*, 2009; *Sugiyama et al.*, 2010], tracks σ_g^2. Note that the trends in σ_g^2 do not follow those of temperature (Figure 1b). To examine the trends in detail we decompose σ_g^2 into separate spatial and temporal components following *Sun et al.* [2010] (Section S1.4 in Text S1). The (linear) trend in σ_g^2 over the 7 decades (1940–2009) is −34.4 (mm month^{-1})^2 decade^{-1} with 1/3 due to a decline in the spatial component (−11.9) and 2/3 due to the temporal component (−22.8) (Table S2 in Text S1). Further, the decline in the temporal component of σ_g^2 is almost entirely due to a decline in the intra-annual component (i.e., seasonal cycle, Figure S13d in Text S1) with only a small residual change in the inter-annual component (Figure S13e in Text S1). The decrease in intra-annual variance could seem counter to an earlier report that the difference between wet and dry season precipitation has increased in the tropics for 1979–2005 [*Chou et al.*, 2007]. Over that shorter period we also find an increase in the intra-annual component (Figures S12b and S13b and Table S4 in Text S1). However, over the full 1940–2009 period, the overall trend in σ_g^2 remains one of decline (Figure 1b and Table S2 in Text S1). The trend in the temporal component of σ_g^2 shows a complex spatial pattern of change (Figure 1e) and regions with increasing mean P (Figure 1d) tend to show increasing P variance (Figure 1e) and vice-versa (Figure S14 in Text S1). However, that simple relation does not adequately explain the overall global result because σ_g^2 decreases whilst μ_g has a near-zero trend (Figures 1a and 1b and Table S2 in Text S1).

[7] The unexpected results prompt the question – what has changed in the P frequency distribution? To address that we develop a generalised space-time probability distribution for P that is related to the sequence of wet and zero-P months. In the monthly (gridded) observations, P rarely equals zero, although it can be close. We define the zero-P using a threshold, P_0. When $P > P_0$ the month is classified as wet, and the wet month frequency ($f_w(P)$) follows the gamma distribution [*Eagleson*, 2002; *Groisman et al.*, 1999; *Karl et al.*, 1995; *Rodríguez-Iturbe and Porporato*, 2004; *Thom*, 1958; *Tsonis*, 1996; *Porporato et al.* 2004]

$$f_w(P) = P^{\alpha-1}\frac{\exp(-P/\beta)}{\Gamma(\alpha)\beta^{\alpha}}, \qquad \text{for } P > P_0 \tag{1}$$

with α the shape parameter controlling the relative contribution from light versus heavy P (Figure S15a in Text S1), $\Gamma(\alpha)$ the factorial gamma function and β (mm month^{-1}) the scale parameter that mostly controls the frequency at the upper P extremes (Figure S15b in Text S1). For zero-P months we use the uniform distribution, $f_d(P) = \frac{1}{P_0}$, for $0 \le P \le P_0$. The mixture distribution is defined by $f(P) = (1 - w)\, f_d(P) + w f_w(P)$ (see Section S2.1 in Text S1), where w (range 0–1) is the number of wet months expressed as a fraction of the total number of months. The mean and variance of the mixture distribution are $\mu = (1 - w)\mu_d + w\,\mu_w$ and $\sigma^2 = (1 - w)\sigma_d^2 + w\sigma_w^2 + w(1 - w)(\mu_w - \mu_d)^2$ respectively [*Wilks*, 2011]. When combined with the definition (equation (1)), the grand mean is

$$\mu_g = (1 - w)\frac{P_0}{2} + w\alpha\beta \approx w\alpha\beta \tag{2a}$$

and the grand variance is

$$\sigma_g^2 = (1 - w)\frac{P_0^2}{12} + w\alpha\beta^2 + w(1 - w)\left(\alpha\beta - \frac{P_0}{2}\right)^2 \approx w\alpha\beta^2(1 + \alpha - w\alpha) \tag{2b}$$

The approximations in equation (2) arise since P_0 is close to, but not exactly, zero. We derived distributions by systematically varying the threshold P_0 between 1 to 2 mm month^{-1}. In all cases, the results were nearly identical and we set the threshold P_0 to be 1 mm month^{-1} (see Section S2.3 in Text S1). The observations follow the mixture distribution (Figure 2 and Figures S16 and S17 in Text S1).

[1] Auxiliary materials are available in the HTML. doi:10.1029/2012GL053369.

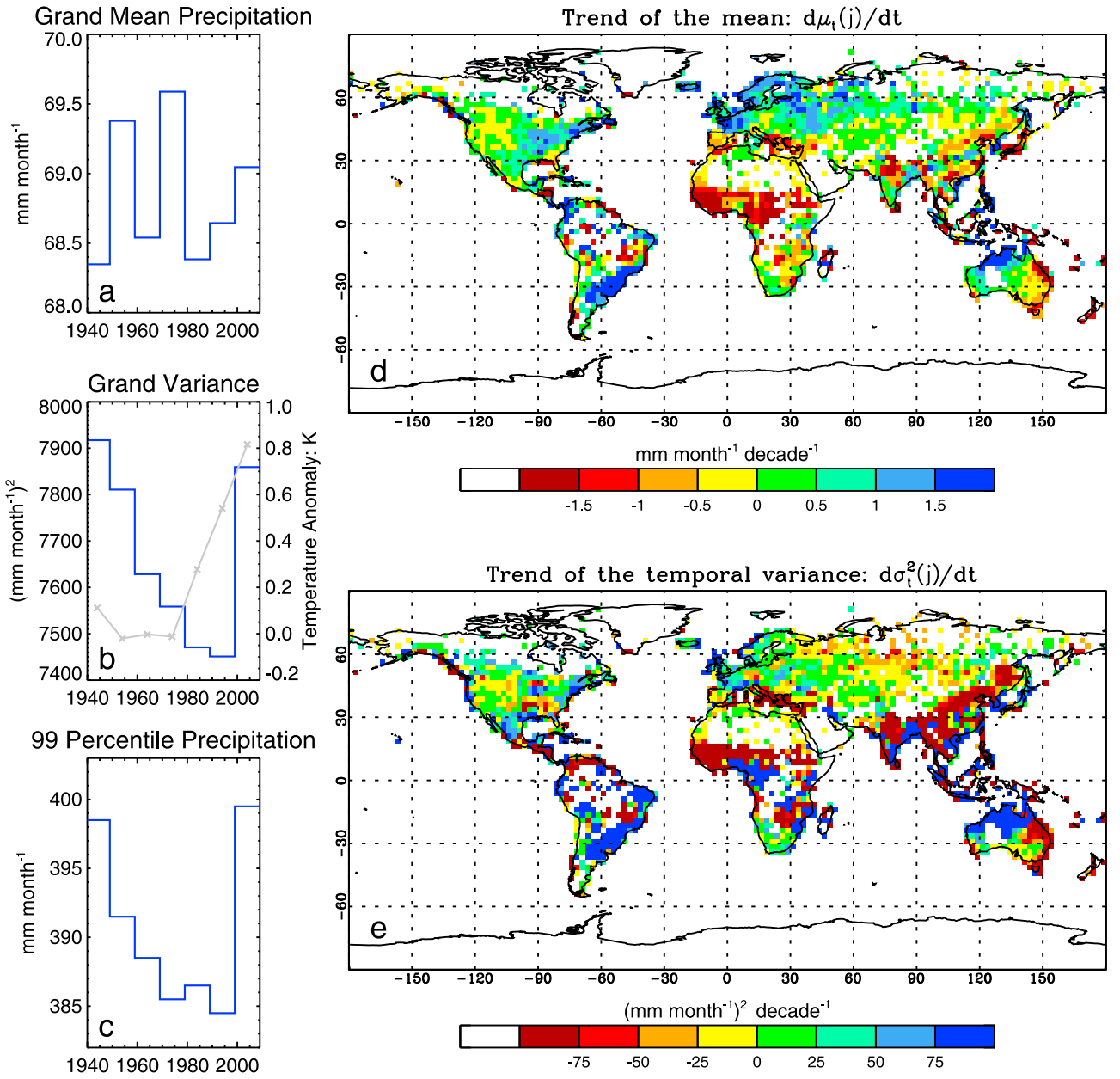

Figure 1. Trends in P variability. Time series of the decadal (a) grand mean (μ_g), (b) grand variance (σ_g^2, blue line) (with temperature anomaly (grey line) from the GISS database [*Hansen et al.*, 2010]), and (c) the 99 percentile of monthly precipitation (GPCC, 1940–2009, with the land mask); and spatial pattern of trends in the (d) mean and (e) temporal variance.

[8] For detection purposes we derive differentials (per equation (2)) for changes in the distribution over successive decades (equations (S6)–(S9) and Section S2.2 in Text S1). First, there is little change in w (Figure 3a). Second, because of the near zero-trend in both w and μ_g (Figure 3b), the observed increase in α must be balanced by an equal and opposite relative decrease in β (Figures 3a and 3b). σ_g^2 is twice as sensitive to the same relative change in β compared to α (equation (S9) in Text S1) and therefore declines (Figure 3c).

[9] The results (Figure 3a) imply a redistribution where P is taken from wet regions/months ($d\beta < 0$) and delivered to dry regions/months ($d\alpha > 0$) (Figure S15c in Text S1). The latitudinal distribution of the observed trend (Figure 4a) and climatology (Figure 4b) are negatively related because P increased in drier zones (e.g., 40°–90°N, 20°–40°S) at the expense of wetter zones (e.g., 0–20°N). That relation is clearer when the trend in P (1940–2009) for each month (in a given grid-box) is grouped into P classes (Figure 4d) and the land area (Figure 4f) is used to adjust the trend to a volumetric basis (Figure 4e). The key result (Figure 4e) shows that P was, on average, removed from relatively wetter regions/months ($P > 100$ mm month^{-1}) with nearly all of that delivered to relatively dry regions/months ($P < 100$ mm month^{-1}). Those results confirm that, on average, dry regions/months became wetter and wet regions/months became drier over the 1940–2009 period. This conclusion holds in all available databases and also holds for 1940–1999 (Figures S18–S24 in Text S1).

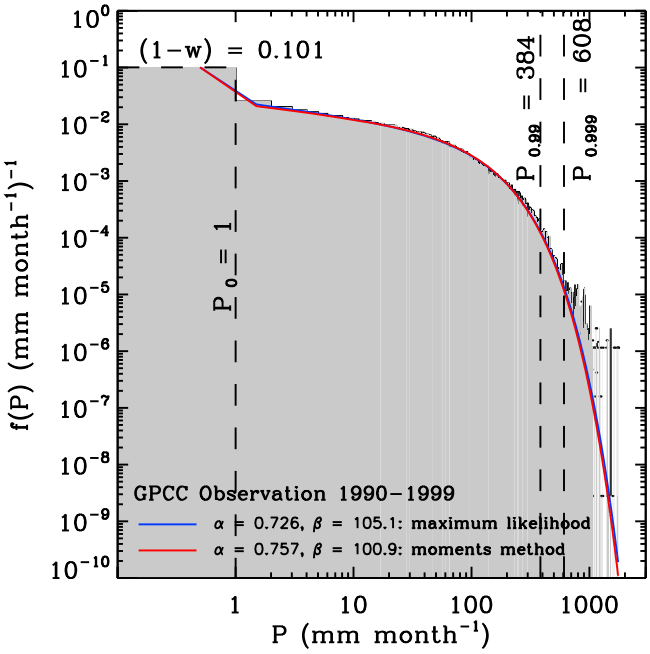

Figure 2. Frequency distribution of decadal *P*. The observations (grey vertical bars at intervals of 1 mm month^{-1}) are fitted by the mixture (uniform-gamma) distribution. The relative frequency of wet months (w) is determined from observations using a threshold (P_0 = 1 mm month^{-1}) and the shape (α) and scaling (β) parameter values (see equation (1)) are estimated using two different methods (maximum likelihood and moments). Empirical estimates of extremes ($P_{0.99}$, $P_{0.999}$) are indicated.

3. Discussion

[10] Early work before the advent of global monthly databases reported increases in monthly *P* variability over much of North America, Europe and Australia [*Tsonis*, 1996] and we found the same pattern (Figure 1e). However, global databases are now available and they reveal many other regions that show decreased *P* variability (Figure 1e). The changes reported here in the (monthly) temporal variance (Figure 1e), that are dominated by the change in the intra-annual variance, reinforce earlier regional studies on changes in daily *P* extremes including increases over much of North America, Europe [*Karl et al.*, 1995; *Min et al.*, 2011], southeastern Brazil [*Teixeira and Satyamurty*, 2011] and South Africa [*Easterling et al.*, 2000a, 2000b; *New et al.*, 2006] alongside declines over many parts of Russia, China [*Karl et al.*, 1995; *Min et al.*, 2011] and Thailand [*Easterling et al.*, 2000a, 2000b] with mixed trends in equatorial Africa [*Easterling et al.*, 2000a, 2000b; *New et al.*, 2006] and India [*Ghosh et al.*, 2011; *Goswami et al.*, 2006]. Importantly, these patterns show no relationship to local (Figure S25 in Text S1) or global changes in temperature (Figure 1b). When integrated there has been little change in global mean *P* over land but with a tendency for dry regions/months to become wetter and wet regions/months to become drier (Figure 4e). This result is robust in all databases examined (Figures S18–S24 in Text S1). If anything, these results constitute a slight decline in meteorological drought over the last 70 years.

[11] Recent climate modelling suggests that *P* extremes and/or variance tend to increase with [CO_2] [*O'Gorman and Schneider*, 2009; *Wetherald*, 2010] but tend to decrease with aerosols [*Chen et al.*, 2011; *Ming and Ramaswamy*, 2011]. Hence a combination of well-mixed greenhouse gases and spatially inhomogeneous aerosols could change local and hemispheric circulations and lead to novel regional impacts [*Bollasina et al.*, 2011; *Rotstayn and Lohmann*, 2002]. In that respect there is a striking spatial correspondence between the largest changes in *P* variability (Figure 1e) and the location of aerosol emissions [*Ramanathan and Feng*, 2009]. This correspondence coupled with modelling studies [*Bollasina et al.*, 2011; *Chen et al.*, 2011; *Ming and*

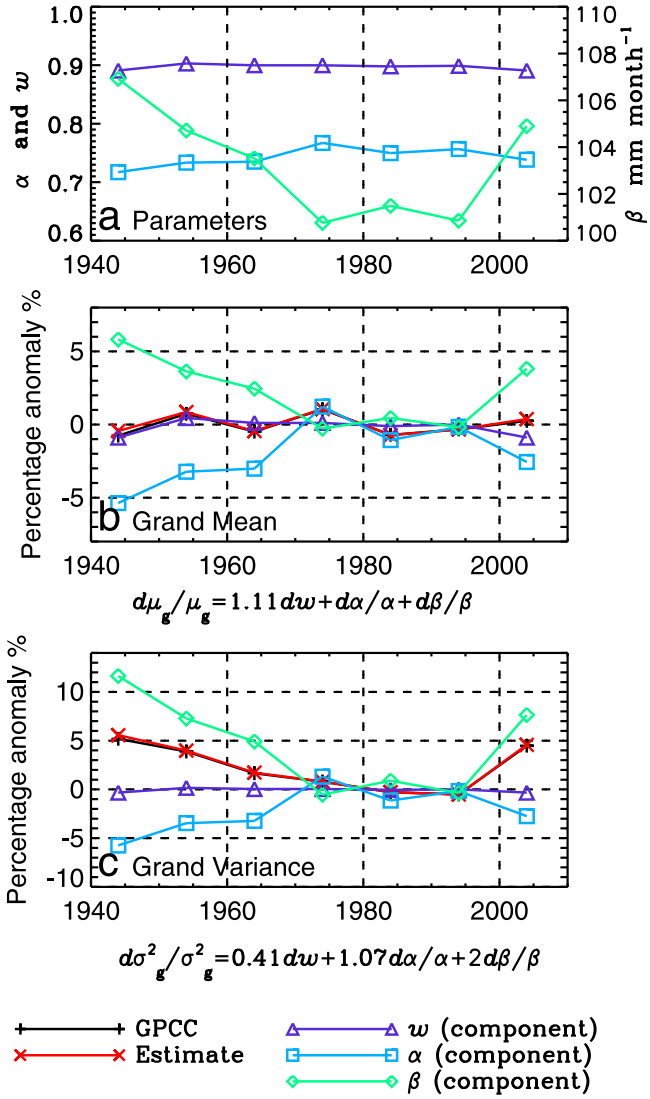

Figure 3. Detection of changes in the global land *P* distribution. (a) Changes in the distribution parameters (in equation (1)) and detection of changes in (b) the decadal grand mean and (c) grand variance. The percentage anomalies are expressed relative to the average for 1970–1999. The total change (GPCC, black line) is estimated (red line) using differentials (shown below Figure 1c). Separate contributions due to changes in the frequency of wet months (w), and the shape (α) and scale (β) parameters of the mixture distribution are depicted.

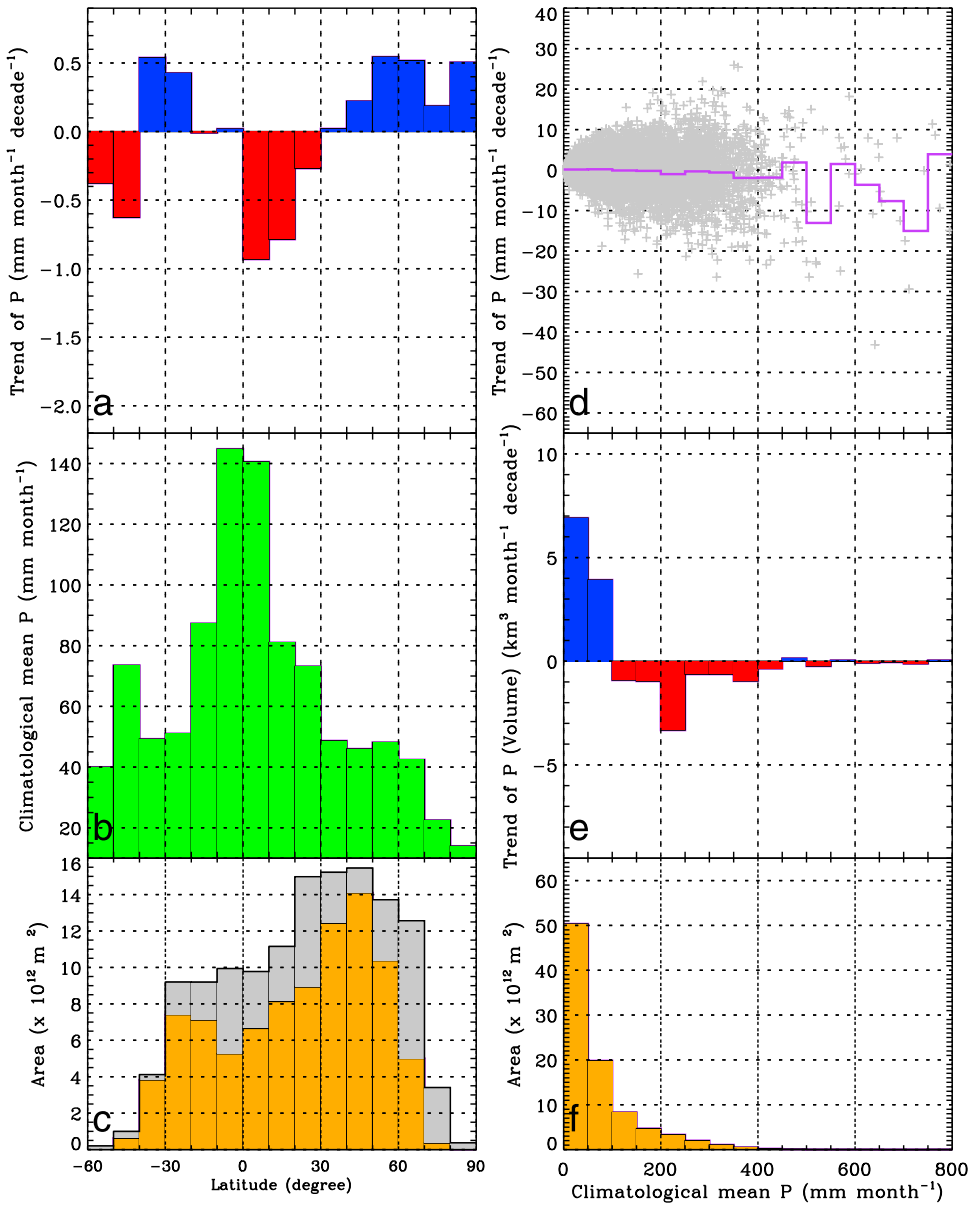

Figure 4. Trends in P in (left) geographic and (right) environmental space for the period: 1940–2009. Regional (latitudinal) distribution of (a) trend in P, (b) climatological mean P and (c) the representative land area (grey denotes the total land area while orange denotes the spatial mask). Local (monthly for each grid-box) trend in P in dimensions of (d) depth (+ denotes a grid-box, line denotes the mean for each 50 mm month^{-1} P class), (e) volume (using liquid water equivalent) weighted by (f) the area of the land mask.

Ramaswamy, 2011; *Rotstayn and Lohmann*, 2002] leads us to speculate that fully accounting for the observed P variability documented here will require intensive investigations to separate the impacts of aerosols and greenhouse gases from natural variability.

[12] **Acknowledgments.** This research was supported by the Australian Research Council (DP110105376, CE11E0098). We thank Dr. Andreas Becker from the Global Precipitation Climatology Centre (GPCC) for providing details about the number of stations in the VASClimO database.

[13] The Editor thanks Yi Ming and an anonymous reviewer for assisting in the evaluation of this paper.

References

Allan, R. P., and B. J. Soden (2008), Atmospheric warming and the amplification of precipitation extremes, *Science*, *321*(5895), 1481–1484, doi:10.1126/science.1160787.

Allen, M. R., and W. J. Ingram (2002), Constraints on future changes in climate and the hydrologic cycle, *Nature*, *419*(6903), 224–232, doi:10.1038/nature01092.

Benestad, R. E. (2006), Can we expect more extreme precipitation on the monthly time scale?, *J. Clim.*, *19*(4), 630–637, doi:10.1175/JCLI3656.1.

Boer, G. J. (2009), Changes in interannual variability and decadal potential predictability under global warming, *J. Clim.*, *22*(11), 3098–3109, doi:10.1175/2008JCLI2835.1.

Bollasina, M. A., Y. Ming, and V. Ramaswamy (2011), Anthropogenic aerosols and the weakening of the South Asian summer monsoon, *Science*, *334*(6055), 502–505, doi:10.1126/science.1204994.

Chen, G., Y. Ming, N. D. Singer, and J. Lu (2011), Testing the Clausius-Clapeyron constraint on the aerosol-induced changes in mean and

extreme precipitation, *Geophys. Res. Lett.*, *38*, L04807, doi:10.1029/2010GL046435.

Chou, C., J. Y. Tu, and P. H. Tan (2007), Asymmetry of tropical precipitation change under global warming, *Geophys. Res. Lett.*, *34*, L17708, doi:10.1029/2007GL030327.

Dai, A., I. Y. Fung, and A. D. DelGenio (1997), Surface observed global land precipitation variations during 1900–88, *J. Clim.*, *10*(11), 2943–2962, doi:10.1175/1520-0442(1997)010<2943:SOGLPV>2.0.CO;2.

Eagleson, P. S. (2002), *Ecohydrology: Darwinian Expression of Vegetation Form and Function*, Cambridge Univ. Press, Cambridge, U. K., doi:10.1017/CBO9780511535680.

Easterling, D. R., G. A. Meehl, C. Parmesan, S. A. Changnon, T. R. Karl, and L. O. Mearns (2000a), Climate extremes: Observations, modeling, and impacts, *Science*, *289*(5487), 2068–2074, doi:10.1126/science.289.5487.2068.

Easterling, D. R., J. L. Evans, P. Y. Groisman, T. R. Karl, K. E. Kunkel, and P. Ambenje (2000b), Observed variability and trends in extreme climate events: A brief review, *Bull. Am. Meteorol. Soc.*, *81*(3), 417–425, doi:10.1175/1520-0477(2000)081<0417:OVATIE>2.3.CO;2.

Ghosh, S., D. Das, S.-C. Kao, and A. R. Ganguly (2011), Lack of uniform trends but increasing spatial variability in observed Indian rainfall extremes, *Nat. Clim. Change*, *2*, 86–91, doi:10.1038/nclimate1327.

Goswami, B. N., V. Venugopal, D. Sengupta, M. S. Madhusoodanan, and P. K. Xavier (2006), Increasing trend of extreme rain events over India in a warming environment, *Science*, *314*(5804), 1442–1445, doi:10.1126/science.1132027.

Groisman, P. Y., et al. (1999), Changes in the probability of heavy precipitation: Important indicators of climatic change, *Clim. Change*, *42*(1), 243–283, doi:10.1023/A:1005432803188.

Hansen, J., R. Ruedy, M. Sato, and K. Lo (2010), Global surface temperature change, *Rev. Geophys.*, *48*, RG4004, doi:10.1029/2010RG000345.

Held, I. M., and B. J. Soden (2006), Robust responses of the hydrological cycle to global warming, *J. Clim.*, *19*(21), 5686–5699, doi:10.1175/JCLI3990.1.

Huffman, G. J., R. F. Adler, D. T. Bolvin, and G. Gu (2009), Improving the global precipitation record: GPCP Version 2.1, *Geophys. Res. Lett.*, *36*, L17808, doi:10.1029/2009GL040000.

Karl, T. R., R. W. Knight, and N. Plummer (1995), Trends in high-frequency climate variability in the twentieth century, *Nature*, *377*(6546), 217–220, doi:10.1038/377217a0.

Min, S.-K., X. Zhang, F. W. Zwiers, and G. C. Hegerl (2011), Human contribution to more-intense precipitation extremes, *Nature*, *470*(7334), 378–381, doi:10.1038/nature09763.

Ming, Y., and V. Ramaswamy (2011), A model investigation of aerosol-induced changes in tropical circulation, *J. Clim.*, *24*, 5125–5133, doi:10.1175/2011JCLI4108.1.

Mitchell, T. D., and P. D. Jones (2005), An improved method of constructing a database of monthly climate observations and associated high-resolution grids, *Int. J. Climatol.*, *25*(6), 693–712, doi:10.1002/joc.1181.

New, M., et al. (2006), Evidence of trends in daily climate extremes over southern and west Africa, *J. Geophys. Res.*, *111*, D14102, doi:10.1029/2005JD006289.

O'Gorman, P. A., and T. Schneider (2009), The physical basis for increases in precipitation extremes in simulations of 21st-century climate change, *Proc. Natl. Acad. Sci. U. S. A.*, *106*(35), 14,773–14,777, doi:10.1073/pnas.0907610106.

Peterson, T. C., and R. S. Vose (1997), An overview of the Global Historical Climatology Network Temperature Database, *Bull. Am. Meteorol. Soc.*, *78*(12), 2837–2849, doi:10.1175/1520-0477(1997)078<2837:AOOTGH>2.0.CO;2.

Porporato, A., E. Daly, and I. Rodriguez-Iturbe (2004), Soil water balance and ecosystem response to climate change, *Am. Nat.*, *164*(5), 625–632, doi:10.1086/424970.

Ramanathan, V., and Y. Feng (2009), Air pollution, greenhouse gases and climate change: Global and regional perspectives, *Atmos. Environ.*, *43*(1), 37–50, doi:10.1016/j.atmosenv.2008.09.063.

Rind, D., R. Goldberg, and R. Ruedy (1989), Change in climate variability in the 21st century, *Clim. Change*, *14*(1), 5–37, doi:10.1007/BF00140173.

Rodríguez-Iturbe, I., and A. Porporato (2004), *Ecohydrology of Water-Controlled Ecosystems: Soil Moisture and Plant Dynamics*, Cambridge Univ. Press, Cambridge, U. K.

Rotstayn, L. D., and U. Lohmann (2002), Tropical rainfall trends and the indirect aerosol effect, *J. Clim.*, *15*(15), 2103–2116, doi:10.1175/1520-0442(2002)015<2103:TRTATI>2.0.CO;2.

Rudolf, B., and U. Schneider (2005), Calculation of gridded precipitation data for the global land-surface using in-situ gauge observations, in *Proceedings of the 2nd International Precipitation Working Group Workshop*, edited by J. Turk and P. Bauer, pp. 231–247, Nav. Res. Lab., Monterey, Calif.

Sugiyama, M., H. Shiogama, and S. Emori (2010), Precipitation extreme changes exceeding moisture content increases in MIROC and IPCC climate models, *Proc. Natl. Acad. Sci. U. S. A.*, *107*(2), 571–575, doi:10.1073/pnas.0903186107.

Sun, F., M. L. Roderick, G. D. Farquhar, W. H. Lim, Y. Zhang, N. Bennett, and S. H. Roxburgh (2010), Partitioning the variance between space and time, *Geophys. Res. Lett.*, *37*, L12704, doi:10.1029/2010GL043323.

Teixeira, M. S., and P. Satyamurty (2011), Trends in the frequency of intense precipitation events in southern and southeastern Brazil during 1960–2004, *J. Clim.*, *24*(7), 1913–1921, doi:10.1175/2011JCLI3511.1.

Thom, H. C. S. (1958), A note on the gamma distribution, *Mon. Weather Rev.*, *86*(4), 117–122, doi:10.1175/1520-0493(1958)086<0117:ANOTGD>2.0.CO;2.

Trenberth, K. E. (2011), Changes in precipitation with climate change, *Clim. Res.*, *47*(1–2), 123–138, doi:10.3354/cr00953.

Trenberth, K. E., A. Dai, R. M. Rasmussen, and D. B. Parsons (2003), The changing character of precipitation, *Bull. Am. Meteorol. Soc.*, *84*(9), 1205–1217, doi:10.1175/BAMS-84-9-1205.

Tsonis, A. A. (1996), Widespread increases in low-frequency variability of precipitation over the past century, *Nature*, *382*(6593), 700–702, doi:10.1038/382700a0.

von Storch, H., and F. W. Zwiers (1999), *Statistical Analysis in Climate Research*, Cambridge Univ. Press, Cambridge, U. K.

Wetherald, R. T. (2010), Changes of time mean state and variability of hydrology in response to a doubling and quadrupling of CO_2, *Clim. Change*, *102*(3–4), 651–670, doi:10.1007/s10584-009-9701-4.

Wilks, D. S. (2011), *Statistical Methods in the Atmospheric Sciences*, 3rd ed., Academic, San Diego, Calif.

Xie, P. P., and P. A. Arkin (1997), Global precipitation: A 17-year monthly analysis based on gauge observations, satellite estimates, and numerical model outputs, *Bull. Am. Meteorol. Soc.*, *78*(11), 2539–2558, doi:10.1175/1520-0477(1997)078<2539:GPAYMA>2.0.CO;2.

Yin, X., A. Gruber, and P. Arkin (2004), Comparison of the GPCP and CMAP merged gauge–satellite monthly precipitation products for the period 1979–2001, *J. Hydrometeorol.*, *5*(6), 1207–1222, doi:10.1175/JHM-392.1.